Conformational stability of amyloid fibrils of β_2-microglobulin probed by guanidine-hydrochloride-induced unfolding

Takehiro Narimoto[a], Kazumasa Sakurai[a], Azusa Okamoto[a], Eri Chatani[a], Masaru Hoshino[a], Kazuhiro Hasegawa[b], Hironobu Naiki[b], Yuji Goto[a,*]

[a] *Institute for Protein Research, Osaka University, and CREST, Japan Science and Technology Corporation, Yamadaoka 3-2, Suita, Osaka 565-0871, Japan*

[b] *Department of Pathological Sciences, Faculty of Medical Sciences, University of Fukui, and CREST, Japan Science and Technology Corporation, Matsuoka, Fukui 910-1193, Japan*

Received 13 August 2004; revised 10 September 2004; accepted 10 September 2004

Available online 25 September 2004

Edited by Gerrit van Meer

Abstract Although the stability of globular proteins has been studied extensively, that of amyloid fibrils is scarcely characterized. β_2-microglobulin (β2-m) is a major component of the amyloid fibrils observed in patients with dialysis-related amyloidosis. We studied the effects of guanidine hydrochloride on the amyloid fibrils of β2-m, revealing a cooperative unfolding transition similar to that of the native state. The stability of amyloid fibrils increased on the addition of ammonium sulfate, consistent with a role of hydrophobic interactions. The results indicate that the analysis of unfolding transition is useful to obtain insight into the structural stability of amyloid fibrils.

Keywords: β_2-Microglobulin; Amyloid fibrils; Protein misfolding; Hydrophobic interaction; Guanidine hydrochloride

1. Introduction

Amyloid fibrils have been recognized to be associated with the pathology of more than 20 serious human diseases, in which the responsible proteins or peptides specific to respective diseases have been identified [1–4]. These fibrils are characterized by a cross-β structure where β-strands are perpendicularly oriented to the axis of the polymeric fibril [5–7]. Moreover, various proteins and peptides that are not related to disease can also form amyloid-like fibrils, implying that the formation of amyloid fibrils is a generic property of polypeptides [4]. Clarifying the conformational stability of amyloid fibrils is essential not only for understanding the pathogenesis of amyloidosis but also for improving our understanding of the mechanism of protein folding.

Many studies have suggested that hydrophobic interactions, important for the formation of the native structures [8], are also essential for the formation of amyloid fibrils [9–13]. On the other hand, the unique cross β-structure specific to amyloid fibrils suggests a fundamental role for hydrogen bonds. Decreasing the net charge tends to stabilize the fibrils, suggesting that the net charge is an additional determinant [9–13]. Considering the marked difference in the morphology of amyloid fibrils and globular proteins, it is likely that the mechanism of the conformational stability of amyloid fibrils is distinct from that of globular proteins even if similar interactions contribute to the stability of amyloid fibrils. The native globular structure is produced by protein evolution in which the optimal packing and concomitant burial of non-polar side chains and polar backbone groups are pursued [8,14]. On the contrary, the amyloid structure of the same polypeptide chain has been suggested to be dominated by the hydrogen-bonded β-sheet architecture of the peptide backbones, consequently, the side chain interactions and packing bearing a secondary role in the structure [4,15]. Therefore, it is important to clarify the similarity and difference between the mechanisms of the conformational stability of native globular states and amyloid fibrils. However, a detailed analysis of stability of the amyloid fibrils has not been carried out.

Dialysis-related amyloidosis is a common and serious complication among patients on long-term hemodialysis, in which β_2-microglobulin (β2-m) forms amyloid fibrils [16]. Native β2-m made of 99 amino acid residues corresponds to a typical immunoglobulin domain (Fig. 1) and is originally a component of type I major histocompatibility antigen [17]. Although an increase in the concentration of β2-m in blood over a long period is the most important risk factor causing amyloidosis, molecular details are unknown. Recently, because of its relatively small size suitable for physicochemical studies, β2-m has become a target of extensive studies for addressing the mechanism of amyloid fibril formation in the context of protein conformation [18–23]. We have been studying the mechanism of fibril formation and conformation with recombinant human β2-m and the fibrils prepared by the seed-dependent extension reaction [24–28].

For small globular proteins, the unfolding transition induced by denaturants such as guanidine hydrochloride (Gdn-HCl) is one of the most useful ways to address the stability of the native state. In this paper, to obtain insight into the conformational stability of amyloid fibrils of β2-m, we studied the unfolding (i.e., depolymerization) of amyloid fibrils induced by Gdn-HCl. The unfolding of fibrils was monitored by examining circular dichroism (CD), tryptophan fluorescence, and thiflavin T (ThT) binding. The results suggest that the

* Corresponding author. Fax: +81-6-6879-8616.
E-mail address: ygoto@protein.osaka-u.ac.jp (Y. Goto).

0014-5793/$22.00
doi:10.1016/j.febslet.2004.09.024

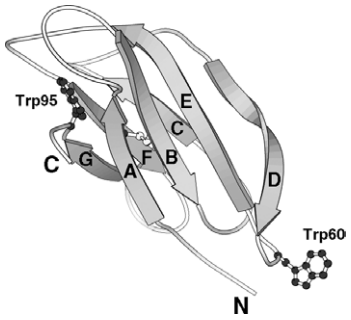

Fig. 1. Structure of β2-m. The locations of tryptophan residues and disulfide bond are indicated. The diagram was created using Molscript [41] with the structure (PDB entry 3HLA) reported by Bjorkman et al. [17].

unfolding transition of amyloid fibrils can be analyzed quantitatively assuming equilibrium between the fibrils and monomers. In addition, the effects of ammonium sulfate indicate that hydrophobic interactions are important for the stability of amyloid fibrils.

2. Materials and methods

2.1. β_2-Microglobulin

Recombinant human β2-m with four residues (Glu–Ala–Tyr–Val–) added at the N-terminal was expressed in the methylotrophic yeast *Pichia pastoris* and purified as described previously [24,25].

2.2. Denaturation of native β2-m by Gdn-HCl

The standard buffers for spectroscopic measurements at pH 7.0 and 2.5 were 50 mM Na phosphate containing 100 mM KCl and 50 mM Na citrate containing 100 mM KCl, respectively. The Gdn-HCl-induced unfolding curves of the native β2-m were obtained from the change of tryptophan fluorescence at 340 nm in the standard buffer (pH 7.0) and 25 °C. We assumed a two-state transition between the native and denatured states. The free energy change of folding (ΔG_f) at a given concentration of Gdn-HCl was described by the standard equation:

$$\Delta G_f = -RT \ln K_f = \Delta G_f(H_2O) + m[\mathrm{GuHCl}], \quad (1)$$

where R, T, $\Delta G_f(H_2O)$, and m are the gas constant, temperature, the free energy change in the absence of Gdn-HCl, and a measure of the cooperativity of folding transition, respectively. The unfolding curves measured by tryptophan fluorescence were normalized assuming appropriate linear baselines for the native and denatured states. Then, the values of $\Delta G_f(H_2O)$ and m were obtained by least-squares fitting to the above equation.

2.3. Polymerization and depolymerization of β2-m

β2-m amyloid fibrils were formed by the fibril extension method as established by Naiki et al. [29], in which the seeds (i.e., fragmented fibrils obtained by ultrasonication) were elongated by monomeric β2-m at pH 2.5 and 37 °C. Unfolding (i.e., depolymerization) of fibrils by Gdn-HCl was measured in 50 M citrate-NaOH buffer (pH 2.5) containing 0.1 M KCl at 25 °C. The kinetics of unfolding was monitored using the ThT assay in 50 mM Na phosphate containing 100 mM KCl at pH 8.0. Then, the solution was incubated overnight and the unfolding of fibrils was monitored by examining the change in the CD spectrum at pH 2.5 and with the ThT assay at pH 8.0. The equilibrium unfolding curves were constructed by measuring the ellipticity at 218 nm or ThT fluorescence assay after overnight incubation at various concentrations of Gdn-HCl at pH 2.5 and 25 °C. The analysis of transition curves is described in Section 4.

2.4. CD and fluorescence measurements

Far-UV CD measurements were performed with a Jasco spectropolarimeter, model J600, at 25 °C using cells with a light path of 1 mm as described previously [24,25]. Fluorescence measurements were performed with a Hitachi fluorescence spectrophotometer, model F-4500, at 25 °C. Fluorescence spectra were measured using a cell with a light path of 5 mm. Tryptophan fluorescence was measured with excitation at 295 nm at a protein concentration of 0.1 mg/ml. In the ThT fluorometric assay of amyloid fibrils, 10 μl of the sample was withdrawn and added to 1 ml of 5 μM ThT solution containing 50 mM Na phosphate (pH 8.0) and 100 mM KCl, and ThT fluorescence was monitored at 485 nm with excitation at 445 nm [29].

3. Results

3.1. Fluorescence and CD spectra of various states

β2-m has two tryptophan residues at positions 60 and 95 (Fig. 1). In the native state, while Trp95 located at the end of β-strand G is partially exposed to the solvent, Trp60 on the β-turn connecting β-strands D and E is largely exposed. The tryptophan fluorescence spectrum of the monomeric β2-m in the buffer at pH 7.0 and 25 °C showed a maximum at 340 nm, consistent with the partial exposure of Trp residues (Fig. 2A). Upon unfolding of β2-m in the presence of 4 M Gdn-HCl at pH 7.0 and 25 °C, the fluorescence intensity decreased and the maximum wavelength showed a red shift to 350 nm, indicating further exposure of tryptophan residues. The far-UV CD spectrum of native β2-m in the absence of Gdn-HCl at pH 7.0 at 25 °C showed a small minimum at 218 nm (Fig. 2B), consistent with previous reports [24–26]. The CD spectrum in 6 M Gdn-HCl is close to that of a random coil, showing that β2-m is largely unfolded.

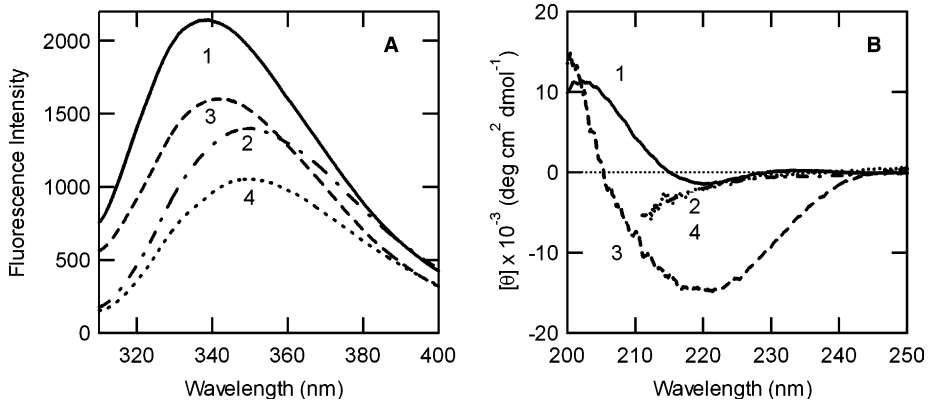

Fig. 2. β2-m in various conformational states is measured by tryptophan fluorescence (A) and CD (B) spectra. 1, Native state at pH 7.0; 2, unfolded state in 6 M Gdn-HCl at pH 7.0; 3, amyloid fibril at pH 2.5; and 4, unfolded state in 6 M Gdn-HCl at pH 2.5.

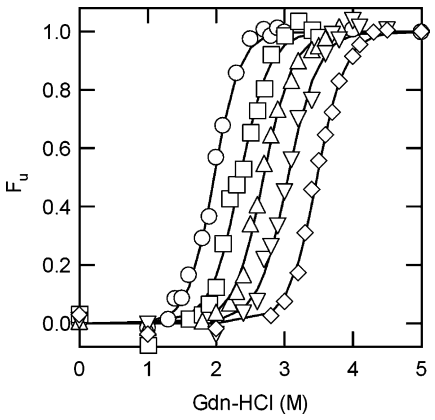

Fig. 3. Unfolding transitions by Gdn-HCl of the native β2-m in the presence of various concentrations of ammonium sulfate at pH 7.0. Concentrations of ammonium sulfate: 0 (circles), 0.3 (squares), 0.5 (triangles), 0.7 (inverted triangles), and 1.0 M (diamonds). The normalized transition curves were constructed with the fluorescence change at 350 nm. The solid lines indicate the theoretical curves on the basis of a two-state mechanism and parameters of Table 1.

Since the fibrils prepared at pH 2.5 depolymerize spontaneously at neutral pH even in the absence of denaturants [30], we studied the stability of fibrils at pH 2.5. The fluorescence spectra of β2-m amyloid fibrils at pH 2.5 showed a maximum at 340 nm and its fluorescence intensity was less than that of the native monomeric state at pH 7.0 (Fig. 2A). In the presence of 6 M Gdn-HCl, the maximum shifted to 350 nm with an accompanying decrease in intensity. The overall change of the spectrum was similar to that of monomeric β2-m, indicating that 6 M Gdn-HCl unfolded the amyloid fibrils. It is noted that the maximal wavelength for the amyloid fibrils in the absence of denaturant is slightly longer than that of the native state, suggesting that the tryptophan residues of amyloid fibrils are more exposed to the solvent than those of the native state.

One of the characteristics of the β2-m amyloid fibrils is the marked intensity of the CD spectrum with a minimum at round 218 nm, suggesting an increased amount of cross β-sheets in comparison with the native state (Fig. 2B). Upon addition of 6 M Gdn-HCl, a dramatic change in the CD spectrum was observed, producing an unfolded state with a spectrum typical of a random coil. The spectrum of amyloid fibrils in 6 M Gdn-HCl was similar to that of monomeric β2-m in 6 M Gdn-HCl at pH 2.5.

3.2. Unfolding transition of the native state

The equilibrium transition curve of the native state at pH 7.0 monitored by tryptophan fluorescence was constructed by measuring the spectrum in the presence of various concentrations of Gdn-HCl (Fig. 3). The unfolding was cooperative, starting at 1.5 M Gdn-HCl with the midpoint at 2.0 M Gdn-HCl. The dilution of Gdn-HCl after incubation of β2-m in 6 M

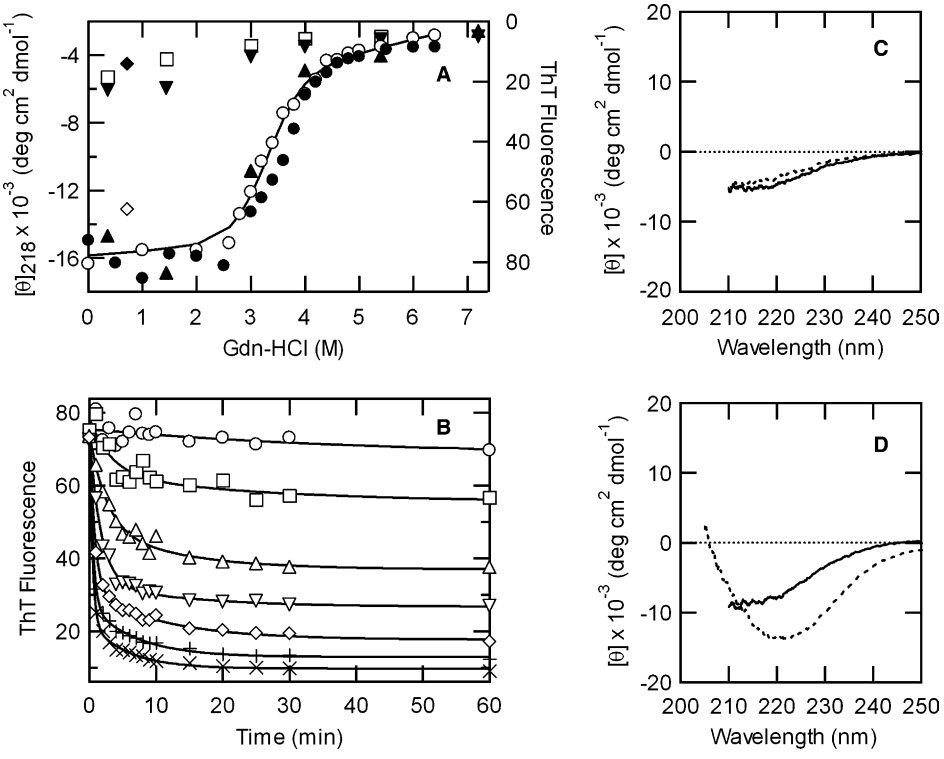

Fig. 4. Unfolding transition by Gdn-HCl of β2-m amyloid fibrils at pH 2.5. (A) Unfolding transitions monitored by CD (open circles) and ThT fluorescence (closed circles). Measurements for checking the reversibility of unfolding were done at about 0 and 12 h after dilution of 7.2 M Gdn-HCl for the samples without centrifugation (closed inverted triangles, 0 h; closed triangles, 12 h), the upper-half fraction (closed diamond) and lower-half fraction (open diamond) after ultracentrifugation (see the text). Open squares represent monomer. The solid curve is a theoretical one constructed with the parameters of Table 1. (B) Kinetics of unfolding monitored by ThT fluorescence. The concentrations of Gdn-HCl are 2.5, 3.0, 3.5, 4.0, 4.5, 5.0, and 5.5 M from top to bottom. (C) For the upper-half fraction after centrifugation of unfolded fibrils in 7.2 M Gdn-HCl, Gdn-HCl was diluted to 0.72 M. Then, the CD spectra were measured 30 min and 12 h after dilution, showing no fibril formation for the completely unfolded fibrils. (D) For the lower-half fraction after centrifugation, Gdn-HCl was also diluted to 0.72 M and the CD spectra were measured 30 min and 12 h later. The spectra showed the fibril formation, suggesting the presence of remaining fibrils and seed-dependent fibril growth.

Gdn-HCl resulted in the full recovery of the native state, showing that the unfolding is reversible (data not shown).

Ammonium ions have been known to stabilize the native structure of proteins by strengthening the hydrophobic interactions [31,32]. The effects are opposite to those of guanidine anion, which weakens hydrophobic interactions. We studied the effects of ammonium sulfate ($(NH_4)_2SO_4$) on the native state by measuring the unfolding transition in the presence of various concentrations of ammonium sulfate. With an increase in the concentration of ammonium sulfate, the transition curve shifted to the higher concentration region of Gdn-HCl. Whereas the midpoint Gdn-HCl concentration of the unfolding was 2.0 M in the absence of ammonium sulfate, it increased to 3.5 M in the presence of 1.0 M ammonium sulfate. The cooperativity of unfolding (i.e., slope of transition region) seemed independent of ammonium sulfate.

It has been shown that the equilibrium unfolding transition of β2-m is approximated by a two-state mechanism between the native and unfolded states [24], although the folding kinetics revealed intermediates [20]. The two-state analysis was performed to obtain the free energy change of folding in the absence of Gdn-HCl ($\Delta G_f(H_2O)$) and the *m* value. In the absence of ammonium sulfate, these values were −25.9 kJ mol^{-1} and 13.2 kJ mol^{-1} (mol of Gdn-HCl)$^{-1}$, respectively. Those in the presence of 1.0 M ammonium sulfate were −41.8 kJ mol^{-1} and 12.0 kJ mol^{-1} (mol of Gdn-HCl)$^{-1}$, respectively. Thus, the presence of 1.0 M ammonium sulfate increased the C_m and $\Delta G_f(H_2O)$ values by 1.5 M and −15.9 kJ mol^{-1}, respectively (Table 1). For comparison, in the case of the C_L fragment of immunoglobulin light chain, another immunoglobulin domain, the increase in $\Delta G_f(H_2O)$ per mole of ammonium sulfate was −15.1 kJ mol^{-1} and the increase in C_m was 1.4 M [31]. The similar values suggest that the effects of ammonium sulfate in increasing the stability are common among various immunoglobulin domains.

3.3. Unfolding of amyloid fibrils

The unfolding transition of amyloid fibrils was measured at pH 2.5 and 25 °C (Fig. 4). Firstly, in order to estimate the incubation time necessary to obtain the transition curve, the kinetics of unfolding in the presence of various concentrations of Gdn-HCl was checked by ThT assay (Fig. 4B). It is noted that the ThT assay is an indirect assay in which the unfolding of amyloid fibrils at pH 2.5 was monitored by assaying the remaining fibrils at pH 8.0. The direct assay at pH 2.5 was not easy because of the decreased intensity of ThT fluorescence at low pH. The ThT assay showed that the amyloid fibrils depolymerized with an increase in the concentration of Gdn-HCl. Apparently, the depolymerization kinetics consists of the major fast phase occurring within a few minutes and the slow phase continuing 10–60 min. Although a detailed analysis of the depolymerization kinetics is difficult at the moment because of the indirect nature of the assay, it is clear that the rate of depolymerization increased with the increase in Gdn-HCl concentration, resulting in a substantial depolymerization in 4 M Gdn-HCl at 1 h.

To construct the equilibrium unfolding transition curve of amyloid fibrils, we incubated the protein solution overnight, more than enough to judge from the kinetic measurement, and the extent of unfolding was measured by CD and ThT assay. Further incubation did not change the transition curve. Intriguingly, the amyloid fibrils at pH 2.5 showed a cooperative unfolding transition both by CD and fluorescence (Fig. 4A). Moreover, the transition curves measured by the two methods agreed with each other. The transition started at 2.5 M Gdn-HCl and ended at around 4.5 M with an apparent midpoint at 3.5 M.

3.4. Reversibility of depolymerization

At pH 2.5 and without seeds, the amyloid fibrils were not formed under our conditions [24,29,30]. It is noted that we did not agitate the solution, so that spontaneous fibril formation as reported by Kad et al. [33] was suppressed. Thus, we anticipated that once the amyloid fibrils were completely unfolded, the dilution of Gdn-HCl does not result in the reformation of amyloid fibrils. Contrary to our expectation, we observed a slow recovery of amyloid fibrils monitored by both CD and ThT assay, establishing the apparent reversibility of fibril unfolding. It is likely that some of the amyloid fibrils resistant to the high concentration of Gdn-HCl remain so as to play the role of a seed.

To examine the presence of remaining seed fibrils in 7.2 M Gdn-HCl, we centrifuged the solution by a BECKMAN optima TLUltracentritage at 100 000 rpm for 180 min at 20 °C, separating the soluble fraction from the fraction which might contain fibrils. The solution after centrifugation was divided into upper and lower fractions and the respective fractions were diluted with 50 mM Na citrate buffer containing 100 mM KCl at pH 2.5 to examine the potential to reform fibrils. After incubation of 24 h at 25 °C, the fibril formation was examined by CD. Only the lower fraction showed the CD spectrum of amyloid fibrils, suggesting the presence of fibrils even after treatment in 7.2 M Gdn-HCl (Fig. 4C and D).

3.5. Effects of ammonium sulfate on amyloid fibrils

The unfolding curves of β2-m amyloid fibrils induced by Gdn-HCl were measured in the presence of various concentrations of ammonium sulfate at 25 °C, which were monitored by the change in CD at 218 nm (Fig. 5). With an increase in the concentration of ammonium sulfate, the unfolding transition

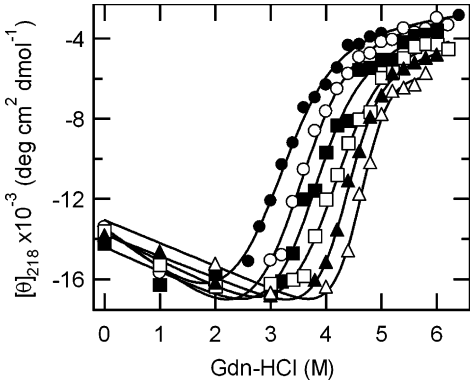

Fig. 5. Unfolding transitions by Gdn-HCl of the amyloid fibrils of β2-m in the presence of various concentrations of ammonium sulfate at pH 2.5. Concentrations of ammonium sulfate: 0 (closed circles), 0.1 (open circles), 0.2 (closed squares), 0.3 (open squares), 0.4 (closed triangles), and 0.5 M (open triangles). The transition curves were constructed with the ellipticity at 218 nm. Normalization was not performed because of the uncertainty of baselines. The solid lines are theoretical curves constructed with Eq. (2), parameters of Table 1, and the indicated base lines.

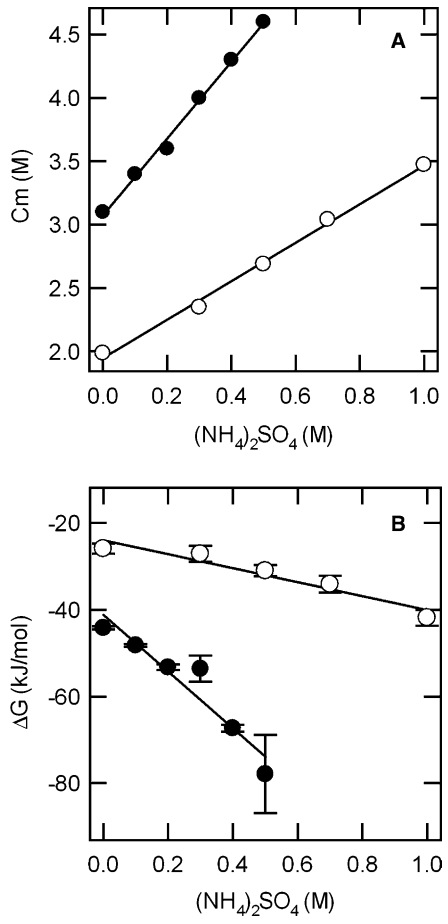

Fig. 6. Dependence of the stability of the native state (○) and amyloid fibril (●) of β2-m on ammonium sulfate. (A) The midpoint concentration of Gdn-HCl-unfolding at pH 7.0. (B) For the native state, ΔG is the free energy change of folding in the absence of Gdn-HCl. For the amyloid fibrils, ΔG for the polymerization process of Scheme 1 in the absence of Gdn-HCl.

of β2-m amyloid fibrils shifted to a higher concentration region of Gdn-HCl. While the Gdn-HCl concentration at the midpoint of unfolding in the absence of ammonium sulfate was 3.1 M, it was 4.6 M in the presence of 0.5 M ammonium sulfate, showing that ammonium sulfate stabilizes the amyloid fibrils. To compare the effect of ammonium sulfate on the amyloid fibrils with that on the native state, the apparent C_m values were plotted against the concentration of ammonium sulfate (Fig. 6). The effects on the amyloid fibrils (3.0 M/(mol of ammnonium sulfate)) were larger than those on the native state (1.5 M/(mol of ammonium sulfate)).

Table 1
Effects of Gdn-HCl and ammonium sulfate on the Gibbs free energy of folding to the native state at pH 7.0 and that of polymerization to amyloid fibrils at pH 2.5, respectively

	$\Delta G(H_2O)$ (kJ/mol)	m (kJ/mol/M)	$d\Delta G(H_2O)/d[(NH_4)_2SO_4]$ (kJ/mol/M)
Folding of monomer	−25.9	13.2	−15.9
Polymerization	−44.2	5.5	−64.6

Yamaguchi et al. [34] reported that heparin, a heterogenous mixture of variously sulfated polysaccharide chains, inhibits the depolymerization of β2-m amyloid fibrils at a neutral pH by direct binding to the fibrils through the negative charges of sulfate groups. The marked effects of ammonium sulfate on the stability of amyloid fibrils suggest that the heparin also stabilizes the amyloid fibrils by a similar mechanism. Since the amount of remaining fibrils in the presence of heparin at neutral pH is not enough to perform the Gdn-HCl-induced depolymerization experiments [34], the Gdn-HCl-induced depolymerization of the fibrils was examined at pH 2.5 in the presence of 3 mg/ml heparin, a concentration much higher than that used by Yamaguchi et al. [34]. However, no stabilizing effect was observed (data not shown), suggesting that heparin was dissociated before the depolymerization of fibrils. Therefore, the present method with Gdn-HCl was not used to examine the stabilizing effects of heparin on amyloid fibrils. Moreover, the results suggest that stabilizing effects of ammonium sulfate are not attributed to the direct binding of sulfate ion, but to affecting the system through perturbing the water structure, thus strengthening the hydrophobic interactions inside the fibrils.

4. Discussion

4.1. Mechanism of unfolding of amyloid fibrils

To address the conformational stability of amyloid fibrils, we measured the Gdn-HCl-dependent unfolding of the amyloid fibrils of β2-m in comparison with that of the native state. In the native state, a cooperative unfolding transition typical of a small globular native protein was observed (Fig. 3). Intriguingly, a similar cooperative transition was also observed for amyloid fibrils (Figs. 4 and 5). However, the interpretation of the unfolding transition of the amyloid fibrils is not straightforward because the unfolding of amyloid fibrils is a complicated process dissociating the polymeric supramolecular structure into monomeric unfolded state. To understand the Gdn-HCl-dependent unfolding of amyloid fibrils, it is essential to consider the mechanism of amyloid fibril formation and the effects of Gdn-HCl on it.

Although the details are still controversial, the basic mechanism of amyloid fibril formation consists of nucleation and growth processes [29,35–37]. One of the simplest models accommodating the two processes is the helical polymerization model proposed by Oosawa and Kasai [38,39], originally used to explain the equilibrium and kinetic features of the globular-to-fibrous transformation of the muscle protein actin. In this model, until the first turn of the helix with j monomers is completed, the addition of each monomer can be described by the same association constant, K_a. Once the second turn starts, each new monomer makes contacts with preexisting subunits rather than one. Hence, the free energy of association will be altered, so that each new addition is governed by a more favorable association constant K_b. The decrease in the stability of amyloid fibrils in the presence of Gdn-HCl might be interpreted in terms of the decrease of K_a and K_b values.

We tried to reproduce the unfolding transition curves on the basis of the helical polymerization model. However, the presence of various adjustable parameters makes the unique determination of these parameters difficult. Moreover, our fitting with the helical polymerization model suggested that K_a and

K_b should not be largely different to reproduce the observed smooth sigmoidal curve of unfolding: if K_b is much larger than K_a the simulated curve will not reproduce the smooth saturating end of the unfolding transition. Therefore, in the present paper, we tentatively assumed that K_a and K_b are the same, reducing the helical polymerization model into a simple linear polymerization model [38,39].

$$\begin{aligned}&[M] + [M] \overset{K_a}{\rightleftarrows} [P_2]\\ &[P_2] + [M] \overset{K_a}{\rightleftarrows} [P_3]\\ &[P_{i-1}] + [M] \overset{K_a}{\rightleftarrows} [P_i]\end{aligned} \qquad \text{(Scheme 1)}$$

where $[M]$, $[P_i]$ is the concentration of monomers and polymer i, respectively, and K_a is the association constant as defined by

$$K_a = \frac{[P_i]}{[P_{i-1}][M]} \tag{2}$$

Thus, the total concentration of β2-m, $[M]_0$, is expressed by

$$[M]_0 = \sum_{i=1}^{\infty} i[P_i] = \sum_{i=1}^{\infty} iK_a^{i-1}[M]^i = \frac{[M]}{(1-K_a[M])^2} \tag{3}$$

Although the scheme might not be the exact one distinguishing the nucleation and growth processes, the advantage is that we can uniquely determine the K_a value. The importance of nucleation and growth processes in amyloid fibril formation is evident. However, it is unknown if the processes are controlled kinetically or by equilibrium. Therefore, our present analysis on the basis of the linear polymerization mechanism will be useful to compare the effects of cosolvents (i.e., Gdn-HCl and ammonium sulfate) to modify the stability of amyloid fibrils.

We assumed that the Gibbs free energy change of association (ΔG_a) increases linearly with the increase in the concentration of Gdn-HCl according to a relationship similar to Eq. (1). Thus, on the basis of Scheme 1 and Eq. (3), the fraction of depolymerization (f_U) can be represented by

$$\begin{aligned} f_U &= \frac{[M]}{[M]_0}\\ &= \frac{2[M]_0 e^{\frac{-\Delta G_a - m[\mathrm{Gdn-HCl}]}{RT}} + 1 - \sqrt{4[M]_0 e^{\frac{-\Delta G_a - m[\mathrm{Gdn-HCl}]}{RT}} + 1}}{2[M]_0^2 \left(e^{\frac{-\Delta G_a - m[\mathrm{Gdn-HCl}]}{RT}}\right)^2} \end{aligned} \tag{4}$$

We first simulated the equilibrium unfolding curve of amyloid fibrils in the absence of ammonium sulfate and estimated the $\Delta G(H_2O)$ and m values to be −44.2 kJ mol^{-1} and 5.5 kJ mol^{-1} (mol of Gdn-HCl)$^{-1}$, respectively. The simulated unfolding curve reproduced the observed curve fairly well (Fig. 4). Then, we simulated the effects of ammonium sulfate, obtaining the $\Delta G(H_2O)$ and m values at respective concentrations of ammonium sulfate. The $\Delta G(H_2O)$ value decreased linearly with the increase in the concentration of ammonium sulfate and its dependence (−64.6 kJ mol^{-1} (mol of ammonium sulfate)$^{-1}$) was larger than that of the native state (Fig. 6B, Tbale 1). The m value showed a slight dependence on the concentration of ammonium sulfate, increasing to 10.9 kJ mol^{-1} (mol of Gdn-HCl)$^{-1}$ at 0.5 M ammonium sulfate.

4.2. Role of hydrophobic and hydrophilic interactions

Consistent with the idea that sulfate ions stabilize the native state by strengthening the hydrophobic interactions, the ΔG_f value of the native state decreased upon addition of ammonium sulfate (Figs. 3 and 6). Similar stabilization by ammonium sulfate was also observed for the amyloid fibrils (Fig. 5). The linear polymerization model suggests that ΔG decreases upon addition of ammonium sulfate (Fig. 6). The importance of hydrophobic interactions in amyloid fibrils has been indicated for several cases showing that the hydrophobicity as well as β-sheet propensity of the key regions and the net charge of the protein are critical for aggregation [9–12].

On the other hand, from the H/D exchange of amide protons of amyloid fibrils monitored by NMR after dissolution of fibrils by dimethylsulfoxide, we indicated that the hydrogen bond network which is more extensive than that of the native state is responsible for the rigidity of amyloid fibrils [26,28]. The extensive hydrogen bond network of the β-structure, more than that of the native globular state, is likely to confer rigidity on the amyloid fibrils and resistance to protease digestion. The observation that amyloid fibrils were completely dissolved by dimethylsulfoxide also supports the importance of hydrogen bonds in the stability of amyloid fibrils [40]. In addition, the depolymerization of the amyloid fibrils at neutral pH regions is consistent with an idea that intricate network of electrostatic interactions including the hydrogen bonds and salt bridges is important.

Taken together, both hydrogen bonds and hydrophobic interactions are important for stabilizing the amyloid fibrils. However, considering the marked difference in morphology, the contribution of the two factors may be different. It has been proposed that while the native states are mainly determined by the tightly packed side-chain interactions, the amyloid fibrils common to various amino acid sequences are formed by the extensively hydrogen bonded main chain cross-β structure [4,15]. Although we cannot evaluate the energetic contribution of the two factors, the contribution of hydrogen bonds should be greater in the amyloid fibrils considering the increased hydrogen bond network in the amyloid fibrils.

In conclusion, we have shown that the unfolding of amyloid fibrils can be treated as a thermodynamic process. However, since the nucleation process and the remaining fibrils after unfolding might affect the observed transition curves, it is important to consider the kinetic factors of the observed transition curves. An exact explanation of the formation and unfolding of amyloid fibrils in terms of thermodynamic terms such as free energy, entropy and enthalpy in comparison with those of the native globular proteins will be needed to clarify the structure and stability of amyloid fibrils.

Acknowledgements: This work was supported by Grants-in-Aid for Priority Areas (15076206, 15032228) and Scientific Research (B) (13480219) from the Japanese Ministry of Education, Culture, Sports, Science and Technology.

References

[1] Sipe, J.D. (1992) Annu. Rev. Biochem. 61, 947–975.
[2] Rochet, J.C. and Lansbury Jr., P.T. (2000) Curr. Opin. Struct. Biol. 10, 60–68.
[3] Cohen, F.E. and Kelly, J.W. (2003) Nature 426, 905–909.
[4] Dobson, C.M. (2003) Nature 426, 884–889.
[5] Serpell, L.C., Sunde, M., Benson, M.D., Tennent, G.A., Pepys, M.B. and Fraser, P.E. (2000) J. Mol. Biol. 300, 1033–1039.
[6] Jimenez, J.L., Nettleton, E.J., Bouchard, M., Robinson, C.V., Dobson, C.M. and Saibil, H.R. (2002) Proc. Natl. Acad. Sci. USA 99, 9196–9201.
[7] Tycko, R. (2003) Biochemistry 42, 3151–3159.

[8] Makhatadze, G.I. and Privalov, P.L. (1995) Adv. Protein Chem. 47, 307–425.
[9] Chiti, F., Calamai, M., Taddei, N., Stefani, M., Ramponi, G. and Dobson, C.M. (2002) Proc. Natl. Acad. Sci. USA 99, 16419–16426.
[10] Calamai, M., Taddei, N., Stefani, M., Ramponi, G. and Chiti, F. (2003) Biochemistry 42, 15078–15083.
[11] Chiti, F., Stefani, M., Taddei, N., Ramponi, G. and Dobson, C.M. (2003) Nature 424, 805–808.
[12] Schmittschmitt, J.P. and Scholtz, J.M. (2003) Protein Sci. 12, 2374–2378.
[13] López de la Paz, M., Goldie, K., Zurdo, J., Lacroix, E., Dobson, C.M., Hoenger, A. and Serrano, L. (2002) Proc. Natl. Acad. Sci. USA 99, 16052–16057.
[14] Fernandez, A., Kardos, J. and Goto, Y. (2003) FEBS Lett. 536, 187–192.
[15] Fändrich, M. and Dobson, C.M. (2002) EMBO J. 21, 5282–5690.
[16] Gejyo, F., Yamada, T., Odani, S., Nakagawa, Y., Arakawa, M., Kunitomo, T., Kataoka, H., Suzuki, M., Hirasawa, Y., Shirahama, T., Cohen, A.S. and Schmid, K. (1985) Biochem. Biophys. Res. Commun. 129, 701–706.
[17] Bjorkman, P.J., Saper, M.A., Samraoui, B., Bennett, W.S., Strominger, J.L. and Wiley, D.C. (1987) Nature 329, 506–512.
[18] Esposito, G., Michelutti, R., Verdone, G., Viglino, P., Hernández, H., Robinson, C.V., Amoresano, A., Dal Piaz, F., Monti, M., Pucci, P., Mangione, P., Stoppini, M., Merlini, G., Ferri, G. and Bellotti, V. (2000) Protein Sci. 9, 831–845.
[19] Monti, M., Principe, S., Giorgetti, S., Mangione, P., Merlini, G., Clark, A., Bellotti, V., Amoresano, A. and Pucci, P. (2002) Protein Sci. 11, 2362–2369.
[20] Chiti, F., Mangione, P., Andreola, A., Giorgetti, S., Stefani, M., Dobson, C.M., Bellotti, V. and Taddei, N. (2001) J. Mol. Biol. 307, 379–391.
[21] Morgan, C.J., Gelfand, M., Atreya, C. and Miranker, A.D. (2001) J. Mol. Biol. 309, 339–345.
[22] McParland, V.J., Kalverda, A.P., Homans, S.W. and Radford, S.E. (2002) Nature Struct. Biol. 9, 326–331.
[23] Ivanova, M.I., Sawaya, M.R., Gingery, M., Attinger, A. and Eisenberg, D. (2004) Proc. Natl. Acad. Sci. USA 101, 10584–10589.
[24] Ohhashi, Y., Hagihara, Y., Kozhukh, G., Hoshino, M., Hasegawa, K., Yamaguchi, I., Naili, H. and Goto, Y. (2002) J. Biochem. 131, 45–52.
[25] Kozhukh, G.V., Hagihara, Y., Kawakami, T., Hasegawa, K., Naiki, H. and Goto, Y. (2002) J. Biol. Chem. 277, 1310–1315.
[26] Hoshino, M., Katou, H., Hagihara, Y., Hasegawa, K., Naiki, H. and Goto, Y. (2002) Nature Struct. Biol. 9, 332–336.
[27] Ban, T., Hamada, D., Hasegawa, K., Naiki, H. and Goto, Y. (2003) J. Biol. Chem. 278, 16462–16465.
[28] Yamaguchi, K., Katou, H., Hoshino, M., Hasegawa, K., Naiki, H. and Goto, Y. (2004) J. Mol. Biol. 338, 559–571.
[29] Naiki, H., Hashimoto, N., Suzuki, S., Kimura, H., Nakakuki, K. and Gejyo, F. (1997) Amyloid 4, 223–232.
[30] Yamaguchi, I., Hasegawa, K., Takahashi, N. and Naiki, H. (2001) Biochemistry 40, 8499–8507.
[31] Goto, Y., Ichimura, N. and Hamaguchi, K. (1988) Biochemistry 27, 1670–1677.
[32] Timasheff, S.N. and Arakawa, T. (1989) in: Protein Structure, A Practical Approach (Creighton, T.E., Ed.), pp. 331–345, Oxford University Press, Oxford.
[33] Kad, N.M., Myers, S.L., Smith, D.P., Smith, D.A., Radford, S.E. and Thomson, N.H. (2003) J. Mol. Biol. 330, 785–797.
[34] Yamaguchi, I., Suda, H., Tsuzuike, N., Seto, K., Seki, M., Yamaguchi, Y., Hasegawa, K., Takahashi, N., Yamamoto, S., Gejyo, F. and Naiki, H. (2003) Kidney Int. 64, 1080–1088.
[35] Scheibel, T., Kowal, A.S., Bloom, J.D. and Lindquist, S.L. (2001) Current Biol. 11, 366–369.
[36] Khurana, R., Ionescu-Zanetti, C., Pope, M., Li, J., Nielson, L., Ramírez-Alvarado, M., Regan, L., Fink, A.L. and Carter, S.A. (2003) Biophys. J. 85, 1135–1144.
[37] Hall, D. and Edskes, H. (2004) J. Mol. Biol. 336, 775–786.
[38] Oosawa, F. and Kasai, M. (1962) J. Mol. Biol. 4, 10–21.
[39] Cantor, C.R. and Schimmel, P.R. (1980) Biophysical Chemistry Part I, The Conformation of Biological Macromolecules. W.H. Freeman and Co, New York.
[40] Hirota-Nakaoka, N., Hasegawa, K., Naiki, H. and Goto, Y. (2003) J. Biochem. 134, 159–164.
[41] Kraulis, P.J. (1991) J. Appl. Crystallogr. 24, 946–950.